JOURNAL OF APPLIED ELECTROCHEMISTRY 2 (1972) 123–136

Zinc passivation and the effect of mass transfer in flowing electrolyte

E. D. FARMER and A. H. WEBB

Central Electricity Generating Board, Research and Development Department, Leatherhead, Surrey, U.K.

Received 28 September 1971

Passivation times, t_p, of a zinc sheet anode have been found to vary from 2 min to 2 h over the experimental range of electrolyte velocities (0·075 to 0·20 ms^{-1}), current densities (3,160 to 1,675 A m^{-2}) and electrolyte temperature (298 to 333 K). For t_p longer than about 40 min there was a change in the nature of the experimental dependence of t_p on the electrolyte flow rate and the current density.

A satisfactory theoretical model of the dissolving zinc anode involving the diffusion of the soluble species through a growing porous solid layer on the electrode surface and through the electrolyte diffusion layer has been formulated to explain the dependence of t_p on the experimental variables.

1. Introduction

The zinc/air battery has received considerable attention in recent years as a potential power source for urban transport vehicles. One of the problems is that at high current densities the zinc anode passivates on prolonged discharge of the battery and thereafter the power available is severely reduced. The time which elapses before passivation depends on the current density, temperature, hydrodynamic and other experimental conditions.

From various studies of zinc anodes in stationary electrolyte, the mechanism of the unpassivated zinc dissolution reaction

$$Zn + 4OH^- \rightarrow [Zn(OH)_4]^{2-} + 2e \quad (1)$$

has been proposed as [1, 2, 3, 4]

$$Zn^* + OH^- \rightarrow [Zn(OH)]^-_{ad} \quad (2)$$

$$[Zn(OH)]^-_{ad} \rightarrow [Zn(OH)]_{ad} + e \quad (3)$$

$$[Zn(OH)]_{ad} + OH^- \rightarrow Zn(OH)_2 + e \quad (4)$$

$$Zn(OH)_2 + 2OH^- \rightarrow [Zn(OH)_4]^{2-} \quad (5)$$

where Zn* refers to a kink site on the metal surface and the subscript 'ad' to a species which is adsorbed onto the surface. From their impedance and electrode transient studies, Farr and Hampson [3, 4] concluded that for small currents, reaction (2) was controlling the dissolution, while at higher polarizations reaction (3) was rate determining.

Popova, Bagotskii and Kabanov [5] concluded that passivation of the zinc electrode occurred when the layer of electrolyte immediately adjacent to the zinc surface reached a critical concentration in zincate. Hampson, Shaw and Taylor [6] reported that their anodic polarization studies indicated that this critical concentration was approximately half the hydroxide ion concentration in the electrolyte. Eisenberg, Bauman and Brettner [7] have measured surface zincate concentrations of this order by blotting the freshly withdrawn electrode on filter paper.

Several workers [6–10] have found that their experimental current density and passivation time measurements in stationary electrolyte could be fitted to an equation of the form

$$(i - i_c) = k t_p^{-\frac{1}{2}} \quad (6)$$

where i is the current flowing, t_p is the passivation time and i_c and k are constants for the

particular system. Application of the laws of unsteady state diffusion to the build-up of the surface concentration of zinc in a semi-infinite medium leads to a current density–time relationship in the form of the Sand equation [11]

$$i = \tfrac{1}{2}z\,\mathrm{F}\sqrt{(\pi D)}\,\Delta C\,t^{-\frac{1}{2}} \qquad (7)$$

where z, F and π have their usual significance, D is the diffusion coefficient of the controlling species (presumed to be the $[Zn(OH)_4]^{2-}$ ion) and ΔC is the concentration difference between the electrode/electrolyte interface and the bulk solution after the time, t. Hampson and his co-workers [6, 9, 10] and Eisenberg *et al.* [7] have explained their experimental results (Equation (6)) by the Sand equation (Equation (7)) with i_c attributed to non-diffusional mass transport (mainly convection) and $k = \frac{1}{2}z\,\mathrm{F}\,\sqrt{(\pi D)}\,\Delta C_{crit}$ where ΔC_{crit} is the critical surface concentration of zinc species required to initiate the formation of the passivating layer. However, under the unstirred electrolyte conditions of their experiments convective transport would vary with time so that i_c would not be a constant independent of t_p.

In studies on the anodic dissolution of zinc, several workers [12–17] have reported the formation of visible solid films on the anode surface which do not however cause passivation directly, but form a physical barrier between the electrode and the bulk electrolyte. These films have a loose porous structure, and may vary in colour from off-white to nearly black depending upon the experimental conditions. The dark colouration has been attributed by Vozdvizhenskii and Kochman [17] to excess zinc atoms contained in the film which originate by disproportionation of monovalent zinc (after reaction (3)):

$$2\,Zn^{I} \rightarrow Zn + Zn^{II}. \qquad (8)$$

Langer and Pantier [14] and Powers and Breiter [15] reported that the surface film is only loosely attached to the zinc surface and may detach as dissolution proceeds.

As passivation of the zinc anode is caused by the attainment of a critical concentration of dissolved zinc at the electrode surface, its onset can be delayed by increasing the mass transport of the dissolved zinc species into the bulk electrolyte. One way of achieving this which has been incorporated in some battery designs [18] is by flowing the electrolyte over the zinc electrode surface. The present work was designed to supplement the published data by providing information on zinc passivation in flowing electrolyte at the longer passivation times relevant to urban transport battery application.

2. Experimental

The perspex laminar flow cell is shown in Fig. 1. Electrolyte, $7{\cdot}0 \pm 0{\cdot}1$ N prepared from technical grade KOH flakes (<2% CO_3^{2-}, <50 ppm Fe) and singly distilled water, was pumped from a thermostatically controlled reservoir through the cell, and returned to the reservoir. The zinc concentration in the electrolyte (total volume approximately 7×10^{-3} m^3) was measured

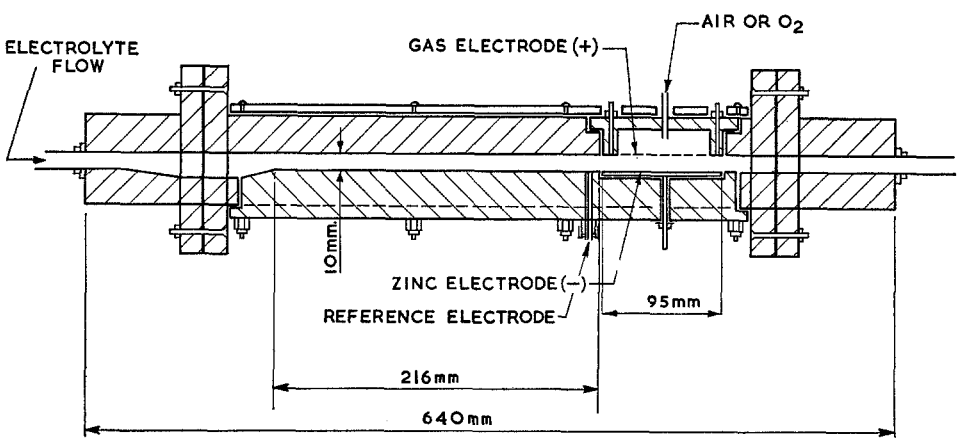

Fig. 1. Laminar flow cell (side view).

periodically by atomic absorption spectrometry, and replaced when the level of zincate approached 0·2 M. The electrolyte flow rate was measured on an orifice meter giving measured flow rates up to 0·33 $m^3 s^{-1}$. The electrolyte flow through the cell was checked for laminar characteristics by injecting a small quantity of potassium permanganate and observing the streamlines.

The zinc electrode (95 mm × 50 mm) was constructed from commercial quality zinc sheet 6·25 mm thick and of 99·4% purity (the principal metallic impurities included 0·6% Pb, 0·025% Fe and 0·006% Cu). The electrode was polished on progressively finer grades of glass paper before insertion in the cell. An oxygen electrode, composed of loosely sintered Ni, Co and Ag powders, was used as the counter electrode, through which oxygen was bubbled at $1·7 \times 10^{-6}$ $m^3 s^{-1}$ at a pressure of $55 \times 10^3 N m^{-2}$ gauge. The cell discharge was controlled by a constant current device and the zinc electrode potential (compared to that of an Hg/HgO reference in the same solution) was measured on a Solartron digital voltmeter of impedance >10 GΩ. The cell voltage was recorded on a chart potentiometer and the normal operating temperature of the cell was 333 K.

The passivation time was measured on a stopclock as the time from closing the circuit to the time when the zinc electrode potential rose to −1·00 V (w.r.t. Hg/HgO) from its open circuit value of about −1·38 V. At −1·00 V the current was switched off; after which the zinc electrode potential then returned to its former open circuit value within about 30 s. To ascertain that no trace of the passivating layer remained, the cell was charged (i.e. the zinc electrode was cathodically polarized) at 200 A m^{-2} at a high electrolyte flow rate for about 10 min. The next measurement of t_p was made after a further 15 min on open circuit to allow the system to reach equilibrium. No significant change in t_p could be detected if the charging period was extended to 20 min.

t_p was measured as the current density, electrolyte flow rate and temperature were varied in turn. Reproducibility of repeated measurements was about ±10% to 20% at the shorter times; but at the longer times where the rate of accumulation of zinc ions at the metal surface is slow, t_p is very sensitive to small changes in the rate of zinc ion mass transport and the deviation between repeated measurements was somewhat larger. The arithmetic mean of several measurements was calculated for each point on the graphs.

3. Experimental results

As has been reported in the literature [12–17], a dark, porous, solid film was formed on the zinc surface during anodic dissolution. It was difficult to determine precisely when this film started to form as it was transparent, especially during the initial stages of its formation. However, it was usually visible within about one or two minutes from starting the run. The exact appearance and nature of this film depended upon the discharge history of the electrode and the electrolyte flow velocity, and it varied in colour from grey to nearly black. At the moment of passivation the major part of the porous film flaked from the electrode surface and was swept away by the flowing electrolyte, leaving a very thin, transparent, bronze-coloured film. Where passivation times exceeded about 15 min some areas of the porous film flaked from the zinc surface during the pre-passivation period. This porous film was obviously very similar to the 'type II' film of ZnO described by Powers *et al.* [15, 23], and in common with these authors, there was no evidence for the formation of 'type I' film under the conditions of stirred electrolyte used.

Gas bubbles were evolved from the surface of the porous film while anodic dissolution was proceeding, and this evolution continued at an appreciable rate even when the electrolyte flow and the cell current were stopped, thus showing that nucleation of gas dissolved in the electrolyte could not be the source. Hydrogen evolution is thermodynamically possible at these potentials; however, the rate of the reaction is slow for a zinc sheet in strong alkali in the absence of a catalyst for the hydrogen evolution reaction [24]. Sanghi and Fleischmann [16] speculated that the zinc oxide film could act as a hydrogen evolution catalyst, and thus the continued gaseous evolution from the film on open circuit could be explained by corrosion cells between the zinc oxide and the excess zinc present in the film.

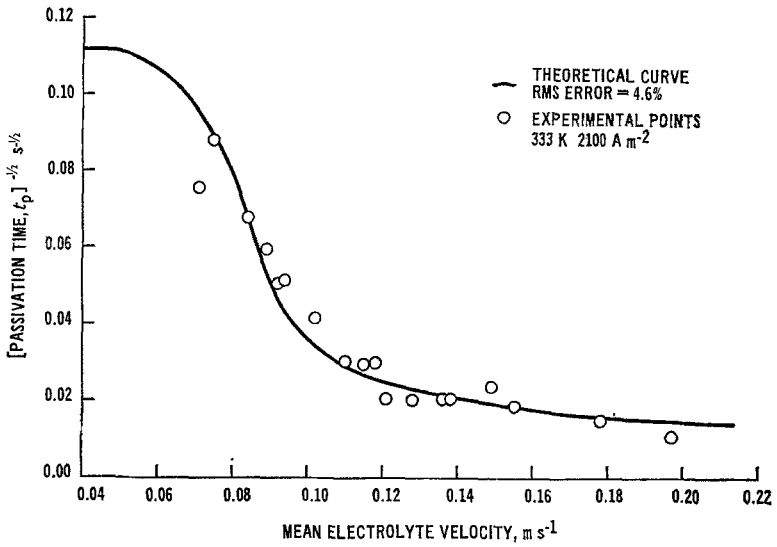

Fig. 2. Experimental and theoretical passivation time versus electrolyte flow rate relationship.

The variation of passivation time with electrolyte flow rate at 333 K and a constant current density of 2,100 A m^{-2} is shown in Fig. 2, plotted as t_p as this affords direct comparison with Fig. 3 and allows the large range of values of t_p (nearly two orders of magnitude) to be shown adequately. At electrolyte velocities less than 0·12 m s^{-1} the passivation time was strongly dependent on the flow velocity—a 50% increase in the electrolyte flow rate produced a tenfold increase in the passivation time. At electrolyte velocities greater than 0·12 m s^{-1} the effect of electrolyte flow rate was less marked—a 50% increase produced only a two- to threefold increase in the passivation time. The transition between these two regions was quite sharp.

The variation of passivation time with current density at 333 K and 0·115 m s^{-1} electrolyte

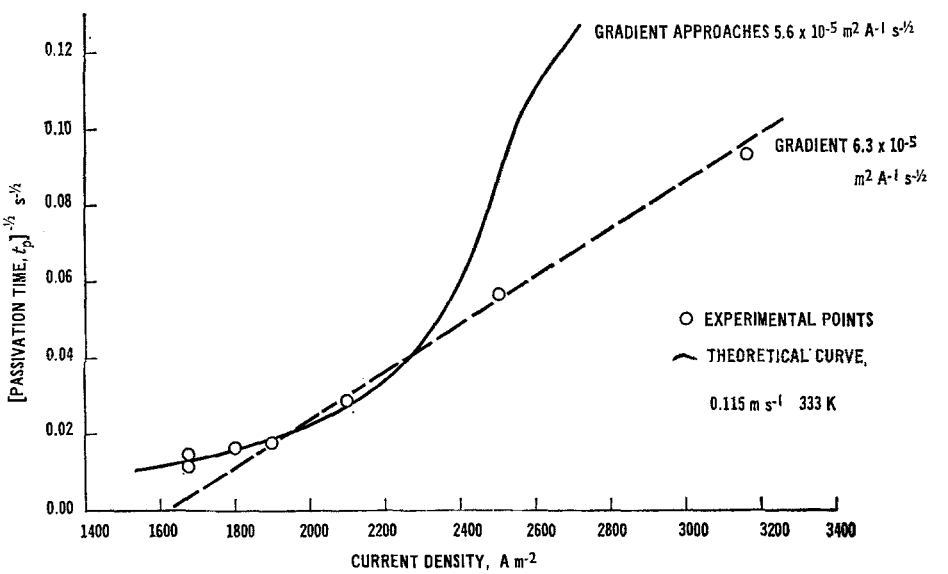

Fig. 3. Experimental and theoretical variation of passivation time with current density.

velocity is shown in Fig. 3 in the form of equation (6). It can be seen from the figure that a straight line (shown dashed in the figure) can be drawn through the points for times up to about 50 min ($t_p \simeq 0{\cdot}019$). For passivation times longer than this, deviation from the linear relationship occurred, the passivation reaction taking place in a shorter time than equation (6) would predict.

Brook and Hampson [19] are the only other workers who have published passivation time data on the anodic dissolution of zinc in a flowing electrolyte system. They used a 99·9995% purity zinc rod with the electrode surface in the vertical plane, and made passivation time measurements in the range $1{\cdot}4 > t_p^{-\frac{1}{2}} > 0{\cdot}2$ (i.e. t_p varied from 0·5 to 25 s). For an electrolyte velocity of 0·11 m s^{-1} at 298 K, their values of the constants in equation (6) would be i_c = 4,500 A m^{-2} and k = 6,500 A m^{-2} $s^{\frac{1}{2}}$. The corresponding values from the present work at 333 K are i_c = 1,630 A m^{-2} and k = 16,000 A m^{-2} $s^{\frac{1}{2}}$. As i_c has been attributed to non-diffusive mass transport we might attempt to explain its reduced value in the present work by the horizontal orientation of the zinc electrode compared to the vertical one of Brook *et al.* In the latter case the electrolyte flow was in an upward direction so that natural density convective flow of the dissolution products would lead to a certain degree of turbulence over the electrode surface. Also, according to Mansfeld and Gilman [20] the presence of Pb^{++} in the electrolyte reduces the number of active sites on the zinc electrode surface for anodic dissolution by deposition of lead atoms, so that passivation might be expected to occur in shorter times with the commercial zinc anodes containing ~0·6% Pb used in this work. The increased value of k in the present work can probably be largely attributed to the higher temperature used and the corresponding increase in the diffusion coefficient, D (see Equation (7)).

The effect of electrolyte temperature on the passivation time at a constant current density of 2,100 A m^{-2} and an electrolyte velocity of 0·115 m s^{-1} is shown in Fig. 4, plotted as $t_p^{-\frac{1}{2}}$ for consistency with Fig. 2 and Fig. 3. Under these conditions the passivation time increased by a factor of approximately seven between 298 K and 333 K.

4. Interpretation

4.1. *The model*

The basis of the model is that the passivating layer is initiated by the attainment of a critical concentration of the zinc ions at the electrode surface, and thus the balance between the rate of the zinc ion formation and the rate of transport of the ions away from the electrode surface into the bulk electrolyte will control the passivation time.

The Sand equation (Equation (7)) which describes the passivation time–current density relationship in unstirred electrolyte when convective

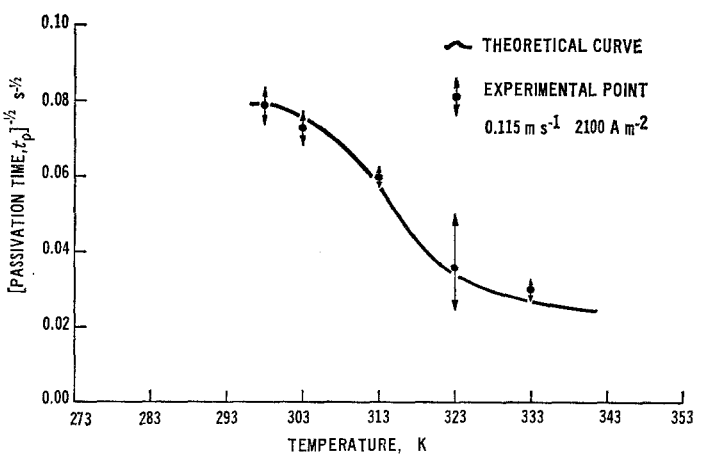

Fig. 4. Experimental and theoretical passivation time versus temperature relationship.

mass transport is negligible, is not applicable to flowing electrolyte conditions. In a flowing electrolyte system operating under laminar flow, with a simple planar solid/liquid interface, the observed mass transport phenomena can be explained, in general, by the assumption of a hypothetical diffusion layer of electrolyte of thickness δ, adjacent to the solid/liquid interface. Mass transport can be assumed to occur exclusively by diffusion across this layer and exclusively by convection outside this layer [21].

In the present case we also have a porous 'oxide' film forming continuously on the electrode surface throughout the time of active dissolution, and this, at least for the longer passivation times, might be expected to have a pronounced effect on the rate of removal of the dissolved zinc into the bulk electrolyte. Thus we might anticipate a change in the electrolyte flow dependence of the passivation time as the relative importance of the 'oxide' film and the electrolyte diffusion layer towards mass transport varies with the electrolyte velocity. Fig. 2 shows that a change does occur in the dependence of t_p on the electrolyte flow rate.

Since this work was started Hull *et al.* [13] have also published work distinguishing between diffusion of soluble zinc species into the bulk electrolyte and transport across the solid surface film under different hydrodynamic conditions.

4.2. *Diffusion through the growing porous 'oxide' layer*

The porous 'oxide' layer may form:

(a) by deposition from the layer of electrolyte immediately adjacent to the electrode surface, e.g.

$$Zn^{2+} + 2OH^- \rightarrow ZnO + H_2O$$

(b) by a concurrent charge transfer reaction, e.g.

$$Zn + 2OH^- \rightarrow ZnO + H_2O + 2e$$

(c) by a simultaneous chemical reaction at the electrode surface, e.g.

$$Zn + H_2O \rightarrow ZnO + H_2$$

In order that we may equate the experimental conditions of constant current with a constant zinc ion flux across the electrode interface we will assume that the surface 'oxide' layer is formed by mechanism (c). However, we will show later (see Section 5.4) that for the specific case of zinc dissolution in strong alkaline solution, the alternative 'oxide' formation reactions would consume a negligible proportion of the ion flux after the first few seconds. We will also assume that the dissolution of the excess zinc in the 'oxide' has a negligible effect on the overall process.

If we assume that the porous 'oxide' may be represented by a homogeneous medium through which the zinc ions diffuse with a constant effective diffusion coefficient, D, and that convective transport of zinc ions through the pores is negligible compared to diffusive transport, Fig. 5 represents the one-dimensional model for removal of soluble zinc species.

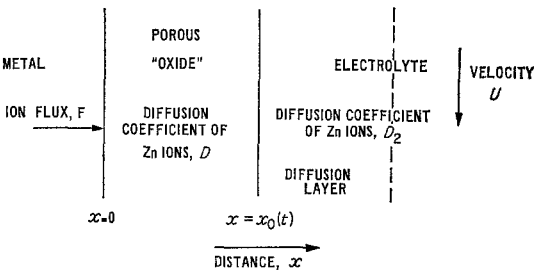

Fig. 5. One-dimensional model of electrode/porous 'oxide'/electrolyte system.

For diffusive transport through the pores of the 'oxide' the concentration of zinc ions satisfies the diffusion equation

$$D\frac{\partial^2 C}{\partial x^2} = \frac{\partial C}{\partial t} \tag{9}$$

and the condition of fixed ion flux F at the electrode interface implies that:

$$-D\left(\frac{\partial C}{\partial x}\right)_{x=0} = F \tag{10}$$

The flux across the moving 'oxide'/electrolyte interface at $x = x_0\ (t)$ is the diffusive flux due to the concentration gradient at the interface, less that due to movement of the interface into the electrolyte.

$$F_{x_0} = -D\left(\frac{\partial C}{\partial x}\right)_{x=x_0(t)} - x'_0(t)[C]_{x=x_0(t)} \quad (11)$$

The quantity F_{x_0} represents the flux leaving the 'oxide' region and entering the electrolyte.

In order to analyse the effect of the moving 'oxide'/electrolyte boundary, $x = x_0(t)$, it is convenient to introduce the new variable y defined by

$$y = \frac{x}{x_0(t)}$$

The diffusion Equation (9) then takes the form:

$$D\frac{\partial^2 C}{\partial y^2} + y\, x_0(t)\, x'_0(t)\frac{\partial C}{\partial y} = x_0^2(t)\frac{\partial C}{\partial t} \quad (12)$$

The condition at the electrode surface (10) becomes

$$\left(\frac{\partial C}{\partial y}\right)_{y=0} = -\frac{Fx_0(t)}{D} \quad (13)$$

and the flux F_{x_0} across the 'oxide'/electrolyte interface (11) is:

$$F_{x_0} = \frac{-D}{x_0(t)}\left(\frac{\partial C}{\partial y}\right)_{y=1} - x'_0(t)\, C_{y=1} \quad (14)$$

We may envisage two idealized growth laws for the thickness of the 'oxide':

(a) if the 'oxide' growth rate is controlled by the rate of diffusion of one of the reactants through the 'oxide' layer, then the 'oxide' thickness will be given by

$$x_0(t) = k_1 t^{\frac{1}{2}}$$

(b) if growth is controlled by the rate of the formation reaction, a linear growth law would be appropriate.

$$x_0(t) = k_2 t$$

Initially we shall consider the $\sqrt{t}$ growth law as this provides a particularly simple case mathematically. In Section 5.4 of this paper we will discuss the effect of the assumption of a linear law, and also the possibility of it being necessary to build up a critical concentration of zinc at the electrode surface before the porous oxide layer starts to form.

As D is assumed to be constant we may write the $\sqrt{t}$ growth law equation in the form

$$x_0(t) = a\sqrt{(Dt)} \quad (15)$$

where 'a' is a dimensionless growth constant.

The quantity $\sqrt{Dt}$ represents approximately the average distance an ion diffuses in a short time t and consequently the growth constant 'a' is the ratio of the distance moved by the 'oxide' front to that moved by a typical ion.

With this growth law the diffusion Equation (12) is

$$\frac{\partial^2 C}{\partial y^2} + \tfrac{1}{2}a^2 y\frac{\partial C}{\partial y} = a^2 t\,\frac{\partial C}{\partial t} \quad (16)$$

The boundary condition at the metal surface (13) is

$$\left(\frac{\partial C}{\partial y}\right) = -aF\sqrt{\left(\frac{t}{D}\right)} \quad (17)$$

and the flux at the 'oxide'/electrolyte interface (14) is

$$F_{x_0} = -\sqrt{\left(\frac{D}{t}\right)}\left[\frac{1}{a}\left(\frac{\partial C}{\partial y}\right)_{y=1} + \tfrac{1}{2}aC_{y=1}\right] \quad (18)$$

It is demonstrated below that the system of Equations (16) and (17) possesses two particularly simple solutions corresponding to concentrations at the 'oxide'/electrolyte interface growing as $\sqrt{t}$ and constant in time, respectively.

(a) '*Oxide*'*/electrolyte interface concentration proportional to* $\sqrt{t}$. In this case the appropriate solution of the diffusion Equation (16) is

$$C = \{\tfrac{1}{2}aAy + B(e^{-\frac{1}{4}a^2y^2} + \tfrac{1}{2}\sqrt{\pi}\, ay\ \mathrm{erf}\ \tfrac{1}{2}ay)\}\, t^{\frac{1}{2}} \quad (19)$$

where A and B are constants determined by the boundary conditions. The condition (17) at the metal surface gives

$$A = -\frac{2F}{\sqrt{D}}$$

and if the 'oxide'/electrolyte interface concentration is denoted by

$$C_{\mathrm{int}} = \frac{F_0 t^{\frac{1}{2}}}{\sqrt{D}} \quad (20)$$

where F_0 is some constant of the dimensions of flux then one finds that

$$B = \frac{(F_0 + aF)}{\sqrt{D}}(e^{-\frac{1}{4}a^2} + \tfrac{1}{2}a\sqrt{\pi}\ \mathrm{erf}\ \tfrac{1}{2}a)^{-1}$$

A further simplification results if we assume that the growth constant 'a' is small compared to unity. This would seem reasonable as 'a' is the ratio of the rate of oxide growth to the rate of ion diffusion and is justified later for zinc dissolution in strong alkali when the model is applied to the experimental results, and 'a' is found to have a value of order 0·02. It is apparent, therefore, that it suffices to evaluate the above expressions to a first order in the quantity 'a' and that second and higher order terms in 'a' may be neglected.

To a first order in 'a' the concentration (Equation (19)) takes the form

$$C = \left\{\frac{F_0}{\sqrt{D}} + \frac{aF}{\sqrt{D}}(1-y)\right\} t^{\frac{1}{2}} \qquad (21)$$

The concentration at the 'oxide'/electrolyte interface (20) is

$$C_{\text{int}} = \frac{F_0 t^{\frac{1}{2}}}{\sqrt{D}} \qquad (22)$$

and the flux at the interface is

$$F_{x_0} = F - aF_0 \qquad (23)$$

(b) *Constant 'oxide'/electrolyte interface concentration.* When the interface concentration is constant in time, the appropriate solution is obtained by setting $A = (-2F)/\sqrt{D}$ and $B = (aF)/\sqrt{D}$ in Equation (19) and adding the constant C_{int} to this solution. The condition $B = (aF)/\sqrt{D}$ ensures that the term in $t^{\frac{1}{2}}$ vanishes at the interface to yield a concentration independent of time. To a first order in the growth constant, 'a', one obtains for the concentration

$$C = \frac{aF}{\sqrt{D}}(1-y)t^{\frac{1}{2}} + C_{\text{int}} \qquad (24)$$

and the flux at the interface is (to a first order) the same as the flux at the metal surface.

$$F_{x_0} = F \qquad (25)$$

The two solutions considered above are both associated with constant flux at the 'oxide'/electrolyte interface. For this reason it is particularly simple to match the solutions to the diffusion process which takes place in the electrolyte.

4.3. *The transport of ions in the electrolyte*

The fluid boundary layer and the diffusion layer thicknesses, δ_0 and δ respectively are related by

$$\delta \simeq \delta_0 / Pr^{1/3}$$

where the Prandtl number, Pr, associated with ion diffusion is given by ν/D_2 where ν is the kinematic viscosity and D_2 is the diffusion coefficient in the electrolyte. This relationship is valid for all velocities as both δ and δ_0 vary as the inverse square-root of the velocity. Typical values of ν and D_2 for aqueous solutions are $\sim 10^{-6}$ m^2 s^{-1} and $\sim 10^{-9}$ m^2 s^{-1} respectively so that $Pr \simeq 10^{-3}$. Hence $\delta \simeq 0{\cdot}1\ \delta_0$ so that the boundary layer concept is valid for this system.

The concentration inside the diffusion layer may be described by the diffusion equation

$$D_2 \frac{\partial^2 C}{\partial x^2} = \frac{\partial C}{\partial t} \qquad (26)$$

The solutions (21) and (24) obtained for the 'oxide' layer both have constant ion flux at the 'oxide'/electrolyte interface. It is appropriate to examine the solution for the concentration in the electrolyte when there is a constant flux entering the fluid.

One wishes to solve the diffusion Equation (26) subject to the conditions

$$\left.\begin{aligned} \left(\frac{\partial C}{\partial x}\right)_{x_0} &= \frac{F_{x_0}}{D_2} \\ \{C\}_{x_0+\delta} &= 0 \end{aligned}\right\} \qquad (27)$$

The latter condition assumes that the ion concentration in the bulk electrolyte is negligible.

The diffusion equation may be solved by expanding the concentration as a Fourier series:

$$C(z,t) = \frac{F_{x_0}}{D_2}\left\{\delta - z - \sum_{n=0}^{\infty} A_n e^{-D_2(n+\frac{1}{2})^2\pi^2 t/\delta^2} \cos(n+\tfrac{1}{2})\frac{\pi z}{\delta}\right\} \qquad (28)$$

where $z = x - x_0$ is the distance from the 'oxide'/electrolyte interface and the 'A_n' are a set of coefficients determined by the condition that the concentration vanishes when $t = 0$.

One has therefore

$$\sum_{n=0}^{\infty} A_n \cos(n+\tfrac{1}{2})\frac{\pi z}{\delta} = \delta - z$$

when $0 \leqslant z \leqslant \delta$ and one finds that

$$A_n = \frac{2\delta}{\pi^2}\,(n+\tfrac{1}{2})^2$$

The concentration at the 'oxide'/electrolyte interface ($z = 0$) is therefore

$$C_{\text{int}}(t) = \frac{F_{x_0}\delta}{D_2}$$

$$\left[1 - \frac{2}{\pi^2}\sum_{n=0}^{\infty}\frac{\exp -D_2\{(n+\tfrac{1}{2})^2\pi^2 t/\delta^2\}}{(n+\tfrac{1}{2})^2}\right] \quad (29)$$

This relation is valid for all times t but at small times it may be shown that the concentration approximates to:

$$C_{\text{int}}(t) \simeq 2F_{x_0}\sqrt{\left(\frac{t}{\pi D_2}\right)} \text{ if } t \ll \delta^2/D_2 \quad (30)$$

On the other hand, at large times the 'oxide'/electrolyte interface concentration approaches the steady value $(F_{x_0}\delta)/D_2$.

4.4. *Ion transport through the oxide and electrolyte diffusion layer*

The two-layer diffusion problem may be solved by combining the 'oxide' and electrolyte concentrations so that both the concentration and flux is continuous across the 'oxide'/electrolyte interface.

For times short compared with the diffusion-layer time-constant, δ^2/D_2, the 'oxide'/electrolyte interface concentration varies as $\sqrt{t}$ (Equation (30)) and thus the appropriate solution is given by Equation (21) with the constant F_0 defined by

$$F_0 = \frac{2F\sqrt{\left(\frac{D}{\pi D_2}\right)}}{1+2a\sqrt{\left(\frac{D}{\pi D_2}\right)}}$$

Hence at short times one finds from Equations (21) and (22) that the concentration at the metal surface (when $y = 0$) is

$$C_{\text{metal}} = \frac{aFt^{\frac{1}{2}}}{\sqrt{D}} + C_{\text{int}} \quad (31)$$

where the 'oxide'/electrolyte interface concentration is

$$C_{\text{int}} = \frac{2Ft^{\frac{1}{2}}}{(\pi D_2)^{\frac{1}{2}}\left(1+2a\sqrt{\left[\frac{D}{\pi D_2}\right]}\right)} \quad (32)$$

and the flux at the 'oxide'/electrolyte interface from Equation (23) is

$$F_{x_0} = F\Big/\left(1+2a\sqrt{\left[\frac{D}{\pi D_2}\right]}\right) \quad (33)$$

At times long compared to δ^2/D_2, the concentration at the 'oxide'/electrolyte interface settles down to its asymptotic value $(F_{x_0}\delta)/D_2$ and the solution given by Equation (24) is applicable. One finds for the concentration at the metal

$$C_{\text{metal}} = \frac{aFt^{\frac{1}{2}}}{\sqrt{D}} + C_{\text{int}} \quad (34)$$

The 'oxide'/electrolyte interface flux equals the flux at the metal (Equation (25))

$$F_{x_0} = F$$

and under these conditions of constant concentration gradient across the diffusion layer the 'oxide'/electrolyte interface concentration is the constant given by

$$C_{\text{int}} = \frac{F\delta}{D_2} \quad (35)$$

Comparison between the short and long time solutions shows that the flux at the 'oxide'/electrolyte interface changes from $F/(1+2a\sqrt{[D/\pi D_2]})$ at short times to F at long times. It is estimated that the ratio of the diffusion coefficients, D/D_2, is of order 10^{-1} and the growth constant is approximately 0·02 (see later) and hence the flux at the interface only increases by about 1% in the transition from short to long times. In addition, comparison of Equations (31) and (34) shows that the short and long time form of the concentration at the metal is identical.

It follows that the concentration at the metal surface is given by Equation (34) at all times and that the 'oxide'/electrolyte interface concentration is given (with negligible error) by the form (from Equation (29))

$$C_{\text{int}} = \frac{\alpha(t) F\delta}{D_2} \times$$

$$\left\{1 - \frac{2}{\pi^2} \sum_{n=0}^{\infty} \frac{\exp - \{D_2 (n+\frac{1}{2})^2 \pi^2 t/\delta^2\}}{(n+\frac{1}{2})^2}\right\} \quad (36)$$

where $\alpha(t)$ is a factor which changes from $(1+2a\sqrt{[D/\pi D_2]})^{-1}$ to unity in the neighbourhood of the time δ^2/D_2.

It follows that the concentrations both on the metal surface and at the 'oxide'/electrolyte interface are readily calculable for all times. The inclusion of the factor $\alpha(t)$ has marginal effect and it will be set equal to unity in the subsequent analysis.

For calculation purposes it is convenient to use normalized quantities.

A length L_0 is defined such that $(L_0 F)/D_2$ is the critical concentration at the metal surface at which passivation occurs. The time-constant of the diffusion layer of thickness L_0 is denoted by τ_0 and $\tau_0 = {L_0}^2/D_2$.

A normalized time θ which quantifies the time in units of the time-constant of the diffusion layer of thickness δ is introduced

$$\theta = D_2 t/\delta^2$$

A velocity U_0 is defined at which the thickness of the diffusion layer is L_0.

At any other velocity U the diffusion layer thickness δ is given by

$$\frac{\delta}{L_0} = \sqrt{\left(\frac{U_0}{U}\right)} \quad (37)$$

Introducing the normalized 'oxide'/electrolyte interface concentration defined by

$$\rho(\theta) = 1 - \frac{2}{\pi^2} \sum_{n=0}^{\infty} \frac{\exp - \{(n+\frac{1}{2})^2 \pi^2 \theta\}}{(n+\frac{1}{2})^2} \quad (38)$$

one finds that the time for passivation, t_p, is determined by solving the relation

$$a\left(\frac{D_2}{D}\right)^{\frac{1}{2}} \theta^{\frac{1}{2}} + \rho(\theta) = \sqrt{\left(\frac{U}{U_0}\right)} \quad (39)$$

and

$$\left.\begin{aligned} \frac{t_p}{\tau_0} &= \frac{U_0}{U}\theta \\ \tau_0 &= \frac{{L_0}^2}{D_2} \end{aligned}\right\} \quad (40)$$

where

If F_0 is a standard ion flux such that $(L_0 F_0)/D_2$ is the critical passivation concentration, the passivation time for any other flux is given by solving

$$a\left(\frac{D_2}{D}\right)^{\frac{1}{2}} \theta^{\frac{1}{2}} + \rho(\theta) = \frac{F_0}{F}\sqrt{\left(\frac{U}{U_0}\right)} \quad (41)$$

Equation (41) determines the passivation time as a function of the flow velocity U and ion flux F.

5. Discussion

5.1. *Passivation time/electrolyte flow rate relationship*

At low flow speeds, the diffusion layer is thick and the passivation time short. In this case from Equation (38) one has

$$\rho(\theta) \simeq \frac{2}{\sqrt{\pi}} \theta^{\frac{1}{2}}$$

The diffusion layer acts under these conditions like a semi-infinite medium and the passivation time reaches a minimum value given by:

$$t_{\min} = \frac{\pi}{4}\tau_0 \quad (42)$$

At high flow speeds, the diffusion layer is thin and the passivation times long. In this case $\rho(\theta) \simeq 1$ and the passivation time, t_p, is given by:

$$\frac{t_p}{\tau_0} = \frac{D}{D_2 a^2}\left(1 - \sqrt{\left[\frac{U_0}{U}\right]}\right)^2$$

As the velocity U increases the passivation time becomes less and less sensitive to velocity changes and it finally reaches a maximum value given by:

$$t_{\max} = \frac{D}{D_2 a^2}\tau_0$$

A small computer program has been written to determine the critical passivation time by solving Equations (39) and (40). The theoretical curve was fitted to the experimental data by determining the velocity scale, U_0, and the time scale, τ_0, so that reasonable agreement was obtained. The results are shown in Fig. 2. The best fit values of the parameters (giving an r.s.m. error of 4·6%) were found to be:

Velocity Scale $U_0 = 0{\cdot}069$ m s^{-1}
Diffusion layer time-constant $\tau_0 = 102$ s
'Oxide' Growth Constant $a = 0{\cdot}0193$ (dimensionless)
Ratio of electrolyte to 'oxide' diffusion coefficients, $D_2/D = 10$

Thus

$$\frac{t_{\max}}{t_{\min}} \simeq 300$$

5.2. *Passivation time/current density relationship (at constant electrolyte flow rate)*

At high current densities the passivation time will be short so that

$$\rho(\theta) \simeq \frac{2}{\sqrt{\pi}}\theta^{\frac{1}{2}} \quad (\theta \ll 1)$$

and one finds that

$$\left(\frac{t_p}{\tau_0}\right)^{-\frac{1}{2}} = \left(\frac{2}{\sqrt{\pi}} + a\sqrt{\left[\frac{D_2}{D}\right]}\right)\frac{F}{F_0} \qquad (45)$$

Thus at high current densities the inverse square root of the passivation time varies linearly with the current density with a slope of

$$\left(\frac{2}{\sqrt{\pi}} + a\sqrt{\left[\frac{D_2}{D}\right]}\right)\Big/ F_0\tau_0^{\frac{1}{2}}.$$

Using the values of the parameters from Section 5.1, this gives a value of $5{\cdot}6 \times 10^{-5}$ m^2 A^{-1} s$^{-\frac{1}{2}}$ while the value of the gradient of the linear region obtained experimentally was $6{\cdot}3 \times 10^{-5}$ m^2 A^{-1} s$^{-\frac{1}{2}}$. Calculation of the full relationship between the current density and $t_p^{-\frac{1}{2}}$ using Equation (41) gives good quantitative agreement between the theoretical and experimental values of t_p only at current densities smaller than 2400 A m^{-2} (Fig. 3). At current densities larger than this value the experimental passivation times were somewhat longer than the model predicted. Also extrapolation of the linear region described by Equation (45) would intersect the axes at the origin. The experimental linear region intersects the current axis at 1630 A m^{-2}. It is thus apparent that as the current density is increased appreciably above the normalized value of 2100 A m^{-2} the assumptions made in the derivation of the model no longer hold true.

At high current densities, very high zinc ion fluxes are developed at the electrode surface, and it is possible that this may affect the initial stages in the porous 'oxide' growth rate, some of the electrochemically dissolved zinc being deposited as oxide, thereby invalidating the assumption of constant ion flux. Thus the passivation time will be longer than the simplified model would predict. However, as the passivation times are still short the effect of the 'oxide' layer on mass transport of the remaining dissolved zinc is negligible, and diffusion layer control is operative. In the analysis we have assumed that the diffusion coefficient is independent of concentration and at these very high current densities and large ion fluxes this assumption may lead to an appreciable error. It is, however, difficult to explain why the experimental points lie on a straight line with an intercept on the current axis unless the linearity is purely fortuitous.

5.3. *Dependence on temperature (at constant current density)*

If we assume that at a standard temperature, T_0, the diffusion coefficient in the electrolyte is D_{2,T_0} and the kinematic viscosity is ν_{T_0}. As the solubility of ZnO in 7 N KOH is little affected by temperature [22] we shall assume that the critical passivation concentration is temperature independent over the small range of temperatures studied experimentally. If we further assume that the ratio of the diffusion coefficients in the 'oxide' and the electrolyte is also independent of temperature, we may show by dimensional analysis that at a temperature, T, with diffusion coefficient $D_{2,T}$ viscosity ν_T and electrolyte velocity U_T the passivation time is equal to $D_{2,T}/D_{2,T_0}$ times the passivation time at the standard temperature, T_0 and flow velocity

$$U_{T_0} = \left(\frac{\nu_{T_0} D_{2,T}^2}{\nu_T D_{2,T_0}^2}\right)^{1/3} U_T$$

Mathematically the passivation time is given by the solution to Equation (41) in the form:

$$a\left(\frac{D_2}{D}\right)^{\frac{1}{2}}\theta^{\frac{1}{2}} + \rho(\theta) = \sqrt{\left(\frac{U_{T_0}}{U_0}\right)}$$

with

$$\frac{t_p}{\tau_{0,T}} = \frac{U_0}{U_{T_0}}\theta$$

and

$$\tau_{0,T} = \frac{D_{2,T}}{D_{2,T_0}}\tau_{0,T_0}$$

where τ_{0,T_0} is the diffusion layer time constant at the standard temperature, T_0.

As the energies of activation of the diffusion processes of similar ions are of the same order, we may obtain approximate relative diffusion coefficients over the experimental temperature range from published diffusion coefficient data. Kinematic viscosity data for 7 N KOH have been published by Hampson *et al.* [10]. The theoretical result is compared to that obtained experimentally in Fig. 4.

5.4. *Other 'oxide' growth rate mechanisms*

So far we have assumed that the porous 'oxide' grows at a rate proportional to $\sqrt{t}$. The good fit between the theoretical $t_p^{-\frac{1}{2}}$ versus current density curve at long times and that obtained experimentally confirms that this is reasonable. The analysis shows that the $\sqrt{t}$ 'oxide' growth law is a critical case where the 'oxide' boundary keeps pace with the ion diffusion process, and the concentration variation in the oxide is approximately linear with distance from the metal surface.

If the 'oxide' growth mechanism were such that the current efficiency for zinc dissolution was less than 100% (see Section 4.2) our assumption of a constant ion flux is not strictly valid. However the 'oxide' growth constant 'a' has a value of approximately 0·02 and by assuming that the oxide porosity is about 60% we can calculate from Equation (15) that after the first 10 s the 'oxide' is consuming less than 10% of the current, and after 2 min the proportion is only about 2%. Thus our assumption of constant ion flux is valid within the accuracy of the model.

The assumption that the 'oxide' grows linearly with time does not affect the minimum passivation time as this is determined entirely by diffusion in the electrolyte (the 'oxide' growth at this stage being negligible). However, as the electrolyte velocity is increased, the passivation time will increase more rapidly than in the $\sqrt{t}$ law case and at long times the oxide/electrolyte boundary movement will so outpace the movement of the ions in the oxide that the behaviour of the system will resemble that with a semi-infinite oxide region.

If a certain concentration of dissolved zinc is required at the electrode interface to initiate the formation of the oxide, then 't' in the oxide growth law equation must be replaced by $(t-t_0)$ where 't_0' is the time required to reach this concentration. t_0 will depend on the mass transfer balance at the electrode surface in much the same way as the passivation time, t_p, in a single electrolyte layer diffusion problem. The good fit of the 't' oxide growth law with the experimental results, and visual observation of the electrode surface during the passivation measurements, leads us to conclude that t_0 was negligible under the conditions of our experiments. As the 'type I' film described by Powers *et al.* [15, 23] is formed by precipitation from super-saturated electrolyte, and would therefore require significant values for t_0, this conclusion implies that the 'type I' film is not a prerequisite for the formation of 'type II' films.

Under experimental conditions for which the delay in the growth of the surface film is significant, the time to passivation may be calculated in the following manner. As shown previously, the ion flux into the electrolyte diffusion layer and the concentration at the oxide/electrolyte interface are virtually independent of the 'oxide' film thickness. Consequently the interface concentration (in units of passivation concentration) is given by the function $\rho(\theta)$ as defined by Equation (38). If ρ_0 is the metal/electrolyte concentration at which growth of the surface film commences, then the time, t_0, at which this occurs is obtained by solving the relation

$$\rho(\theta_0) = \rho_0$$

for θ_0 and calculating t_0 using:

$$t_0 = \frac{L_0^2 U_0 \theta_0}{D_2 U}$$

The thickness of the oxide film at times greater than t_0 obeys the law

$$x_0(t) = a\sqrt{(D[t-t_0])}$$

and the passivation time is obtained by solving the relation (analogous to Equation (39))

$$a\left(\frac{D_2}{D}\right)^{\frac{1}{2}}(\theta-\theta_0)^{\frac{1}{2}}+\rho(\theta) = \sqrt{\left(\frac{U}{U_0}\right)}$$

The effect of this modification to the 'oxide' growth law is readily deduced. For short passivation times, diffusion in the electrolyte is dominant and no significant change to the passivation time will occur. For long passivation times, the delayed growth of the 'oxide' film will cause the passivation time to increase by a maximum amount equal to the delay time, t_0. The transition between these two regimes occurs at times comparable with the diffusion layer time-constant τ_0 (given in Section 5.1 as 102 s). It follows that, to be significant, the delay time t_0 must be a substantial fraction of τ_0.

An oxide growth law of the form $x_0(t) = k_2(t-t_0)$ can be treated in a similar manner to the above.

6. Conclusions

(1) The passivation time was strongly dependent upon the electrolyte flow rate, a 50% increase in the flow producing up to a tenfold increase in the passivation time. The effect of electrolyte flow on the passivation time was more marked at low flow velocities and short passivation times.

(2) The formulated model has good quantitative agreement with experiment under constant current conditions. The system may therefore be understood in terms of the diffusion of dissolved species through a growing porous solid layer on the electrode surface and through the electrolyte diffusion layer.

(3) The model predicts a linear relationship between the inverse square root of the passivation time and the current density at short times. While the high current density experimental points lay approximately on a straight line of the correct slope, quantitative agreement at high currents was poor—indicating that the system parameters are current dependent at these high ion fluxes.

(4) The model affords an adequate description of the mass transport processes at long times so that the $\sqrt{t}$ 'oxide' growth law is substantially correct. Under this law, the model is admissible to simple analytical solution which allows good quantitative predictions to be made.

7. Acknowledgments

The authors would like to thank Dr N. S. Wrench who initiated the flowing electrolyte experiments, Mr A. F. Cook for his practical assistance and Dr A. J. B. Cutler for helpful discussions.

This work was carried out at the Central Electricity Research Laboratories, Kelvin Avenue, Leatherhead, and is published by permission of the Central Electricity Generating Board.

8. References

[1] H. Gerischer, *Z. Physik. Chem.*, **43** (1953) 845.
[2] T. P. Dirkse, *J. Electrochem. Soc.*, **102** (1955) 497.
[3] J. P. G. Farr and N. A. Hampson, *Trans. Faraday Soc.*, **62** (1966) 3493.
[4] J. P. G. Farr and N. A. Hampson, *J. Electroanal. Chem.*, **13** (1967) 433.
[5] T. I. Popova, V. S. Bagotskii and B. N. Kabanov, *Russ. J. Phys. Chem.*, **36** (1962) 766.
[6] N. A. Hampson, P. E. Shaw and R. Taylor, *Br. Corr. J.*, **4** (1969) 207.
[7] M. Eisenberg, H. F. Bauman and D. M. Brettner, *J. Electrochem. Soc.*, **108** (1961) 909.
[8] H. Bartelt and R. Landsberg, *Z. Physik. Chem.*, **222** (1962) 217.
[9] N. A. Hampson and M. J. Tarbox, *J. Electrochem. Soc.*, **110** (1963) 95.
[10] N. A. Hampson, M. J. Tarbox, J. T. Lilley and J. P. G. Farr, *Electrochem. Tech.*, **2** (1964) 309.
[11] H. J. S. Sand, *Phil. Mag.*, **1** (1901) 45.
[12] K. Huber, *J. Electrochem. Soc.*, **100** (1953) 376.
[13] M. N. Hull, J. E. Ellison and J. E. Toni, *J. Electrochem. Soc.*, **117** (1970) 192.
[14] A. Langer and E. A. Pantier, *J. Electrochem. Soc.*, **115** (1968) 990.
[15] R. W. Powers and M. W. Breiter, *J. Electrochem. Soc.*, **116** (1969) 719.
[16] I. Sanghi and M. Fleischmann, *Electrochim. Acta*, **1** (1959) 161.
[17] G. S. Vozdvizhenskii and E. D. Kochman, *Russ. J. Phys. Chem.*, **39** (1965) 347.
[18] e.g. P. R. Shipps, *Proc. Ann. Power Sources Conf.* (1966) 86.

[19] M. J. Brook and N. A. Hampson, *Electrochim. Acta*, **15** (1970) 1749.
[20] F. Mansfeld and S. Gilman, *J. Electrochem. Soc.*, **117** (1970) 588.
[21] V. G. Levich, 'Physiochemical Hydrodynamics' (1962) Prentice-Hall (New York).
[22] T. P. Dirkse, *J. Electrochem. Soc.*, **106** (1959) 154.
[23] R. W. Powers, *J. Electrochem. Soc.*, **116** (1969) 1652.
[24] N. A. Hampson, Private Communication (1969).